National Conference with International Participation
ENGINEERING MECHANICS 2003
Svratka, Czech Republic, May 12 – 15, 2003
paper no. 315

NUMERICAL SOLUTION OF PROBLEMS OF FINITE HYPERELASTICITY

A. Poživilová*

Summary: *Hyperelastic material model based on the logarithmic description is implemented in the finite element code. Procedure for the calculation of all the necessary quantities at the Gauss integration points is described in details. The second-rank update BFGS solver is used to process the governing equilibrium equations. The solution algorithm is then combined with the pre-discretization contact search method in order to include contact boundary conditions. As an example, numerical simulation of the compression test of a rubber cylindrical specimen is presented.*

1. Introduction

For the verification of the hyperelastic constitutive model the simulations of experimens have to be compared with measured data. The experimental data from simple homogeneous load modes can be compared with analytical solutions, but more complex deformations must be solved with approximate numerical methods. A very popular numerical method for solving nonlinear mechanical problems is the finite element method (FEM).

Proposed constitutive model was based on the linear relation between the logarithmic strain tensor and its conjugate stress tensor. Details about this constitutive model can be found in [Poživilová 2002] or [Poživilová and Plešek 2002].

The main emphasis in this text is given to the implementation of the constitutive relation to the existing FEM solver and the choice of the numerical method. For the nonlinear problems, the governing equations are given, together with the algorithm of the computation of the stress in the Gauss integration point for proposed constitutive model. The advantages of the use of the second rank update BFGS solver for solution of the nonlinear system of equations are discussed. In the end of this text, the numerical simulation of the compression test of the rubber cylinder is presented.

*Ing. Alena Poživilová, Ph.D.: Institute of Thermomechanics, Academy of Sciences of the Czech Republic; Dolejškova 5; 182 00 Praha 8; tel. +420 266 053 792; fax: +420 285 584 695; email: alena@it.cas.cz

2. Governing equations

Numerical solution of problems of the rubber elasticity requires adequate dealing with not only material, but also geometrical nonlinearities. Identically to the linear problems, the governing equations covering the nonlinear problems are obtained from the principle of virtual displacement. This principle states that for any compatible small virtual displacement imposed on the body in its state of equilibrium, the total internal virtual work is equal to the total external virtual work.

Static equilibrium is described by the equation of equilibrium

$$\operatorname{div}(\boldsymbol{\sigma}) + \mathbf{b} = \mathbf{0} \qquad \text{in } {}^{t}V \qquad \text{with the boundary condition } \boldsymbol{\sigma}\mathbf{n} = \mathbf{t} \qquad \text{on } {}^{t}\Gamma_{\mathrm{S}} \tag{1}$$

$\boldsymbol{\sigma}$ is the Cauchy stress tensor, $\mathbf{b}$ is the vector of the body forces and $\mathbf{t}$ are tractions on the surface.

The weak form of this equation

$$\int_{{}^{t}V} \delta\mathbf{u}^{\mathrm{T}} \left[\operatorname{div}(\boldsymbol{\sigma}) + \mathbf{b}\right] \mathrm{d}V = 0 \tag{2}$$

is called the principle of virtual displacement. δ denotes the variation of the quantity and $\delta\mathbf{u}$ is the virtual displacement. Expanding the first term by the product rule and then rearranging by means of the Greens's theorem we obtain the principle of virtual displacement in the form

$$\int_{{}^{t}V} \delta\boldsymbol{\epsilon} : \boldsymbol{\sigma} \, \mathrm{d}V - \int_{{}^{t}V} \delta\mathbf{u}^{\mathrm{T}}\mathbf{b} \, \mathrm{d}V - \int_{{}^{t}\Gamma_{\mathrm{S}}} \delta\mathbf{u}^{\mathrm{T}}\mathbf{t} \, \mathrm{d}S = 0 \tag{3}$$

where $\delta\boldsymbol{\epsilon}$ denotes the variation of the strain tensor $\delta\boldsymbol{\epsilon} = \frac{\partial(\delta\mathbf{u})}{\partial\, {}^{t}\mathbf{x}}$. Considering large strains, the difference between the original and current configuration cannot be neglected and all the integrations must be performed over the deformed size of volume of the body.

In the finite element method, the body is divided in the system of elements, which are all in equilibrium. For the assemblage of finite elements we rewrite the equilibrium equation (3) as a sum of integration over volumes and areas of all finite elements. The continuum displacement field $\mathbf{u}$ is replaced in every element by its approximation $\mathbf{u}^{(e)} = \mathbf{H}^{(e)}\hat{\mathbf{u}}^{(e)}$, where $\mathbf{H}^{(e)}$ are so called shape functions dependent upon the employed type of element and $\hat{\mathbf{u}}^{(e)}$ is the vector of the displacement components at all nodal points of the e-th element. This does not differs from the spatial discretisation of the principle of virtual power for solution of linear problems. The strain vector $\boldsymbol{\epsilon}^{(e)}$ is determined by the kinematic relation $\boldsymbol{\epsilon}^{(e)} = {}^{t}\mathbf{B}^{(e)}\hat{\mathbf{u}}^{(e)}$. The strain-displacement matrix ${}^{t}\mathbf{B}^{(e)}$ is obtained by appropriate differentiating of components of $\mathbf{H}^{(e)}$ in respect to the current coordinates.

To enable the direct calculation of the finite element matrices, the isoparametric elements were used. At every element the element coordinates $\mathbf{x}^{(e)}$ are expressed in the form of the interpolations of the nodal coordinates $\hat{\mathbf{x}}^{(e)}$ according to the relation $\mathbf{x}^{(e)} = \mathbf{H}^{(e)\,\mathrm{T}}\hat{\mathbf{x}}^{(e)}$. Both matrices $\mathbf{H}^{(e)}$ and ${}^{t}\mathbf{B}^{(e)}$ are expressed in non-dimensional coordinates $\mathbf{r}^{(e)}$. The operator relating the non-dimensional coordinate derivatives to the global

coordinates derivatives is called Jacobian and is defined as $\mathbf{J}^{(e)} = \frac{\partial\, {}^t\mathbf{x}^{(e)}}{\partial\, \mathbf{r}^{(e)}}$. Accepting that the equation (3) must holds for an arbitrary virtual displacement $\delta\mathbf{u}$ we obtain the system of equation governing the nonlinear mechanical problem

$$\sum_{e=1}^{k} \int\limits_{{}^tV^{(e)}} \det \mathbf{J}^{(e)}\ {}^t\mathbf{B}^{(e)\,\mathrm{T}} \vec{\boldsymbol{\sigma}}\, \mathrm{d}r_1^{(e)}\, \mathrm{d}r_2^{(e)}\, \mathrm{d}r_3^{(e)} = \sum_{e=1}^{k} \int\limits_{{}^tV^{(e)}} \det \mathbf{J}^{(e)}\, \mathbf{H}^{(e)\,\mathrm{T}} \mathbf{b}^{(e)}\, \mathrm{d}r_1^{(e)}\, \mathrm{d}r_2^{(e)}\, \mathrm{d}r_3^{(e)} + \\ + \sum_{e=1}^{k} \int\limits_{{}^t\Gamma_1, {}^t\Gamma_2 \ldots} \det \mathbf{J}_{\mathrm{S}}^{(e)} \mathbf{H}^{(e)\,\mathrm{T}} \mathbf{t}^{(e)}\, \mathrm{d}S(\mathbf{r})^{(e)} + \sum_{e=1}^{k} \mathbf{f}^{(e)} \quad (4)$$

where $\vec{\boldsymbol{\sigma}}$ denotes the stress vector built from the elements of Cauchy stress tensor. The left side of the equation is called internal force vector and the right side of the equation is called external force vector.

3. Solution of nonlinear equations

Once the nonlinear system of equations (4) is established, it is necessary to find its solution. Its character is inherently nonlinear and the nonlinear solver must be used. The solution can be divided into three steps

1. Evaluate the internal forces vector $\mathbf{f}_{\mathrm{int}}$ for the given approximation to the solution $\hat{\mathbf{u}}_n$. The integration is carried over the current domain ${}^tV$.
2. Evaluate the residual vector $\mathbf{g}_n$ as the difference between the internal and external equivalent forces. The residual vector $\mathbf{g}_n$ is also known as the gradient of the total potential energy due to displacements $\hat{\mathbf{u}}_n$.
3. On the basis of information drawn form the last few iterations set a new approximation $\hat{\mathbf{u}}_{n+1}$ and repeat the cycle until the convergence is reached.

The most important part of the computation of internal nodal forces is the evaluation of the stress $\vec{\boldsymbol{\sigma}}$ in every Gauss integration point. The stress is given by the particular constitutive equations. In our problems we use for the description of constitutive behaviour of rubber the logarithmic strain tensor for the description of displacement. The relation between the logarithmic strain and stress tensor conjugate with this strain tensor was linear.

The procedure for the computation of the internal nodal forces

$$\mathbf{f}_{\mathrm{int}}^{(e)} = \int\limits_{{}^tV^{(e)}} \det \mathbf{J}^{(e)}\ {}^t\mathbf{B}^{(e)\,\mathrm{T}} \vec{\boldsymbol{\sigma}}\, \mathrm{d}r_1^{(e)}\, \mathrm{d}r_2^{(e)}\, \mathrm{d}r_3^{(e)} \quad (5)$$

for the proposed constitutive model is given in Box 1.

In the equilibrium state the internal force vector equals to the external force vector. The difference between the internal and external equivalent forces for the n-th approximation of the solution $\mathbf{u}_n$ is called a residual vector

$$\mathbf{g}(\mathbf{u}_n) = \mathbf{f}_{\mathrm{int}} - \mathbf{f}_{\mathrm{ext}} \quad (6)$$

Internal nodal force computation for element

- $\mathbf{f}_{\text{int}} = 0$
- for all quadrature points of the e-th element
  - compute strain-displacement matrix ${}^0\mathbf{B}_n^{(e)}$
  - compute displacement gradient $\mathbf{H}_n$
  - compute deformation gradient $\mathbf{F}_n = \mathbf{I} + \mathbf{H}_n$
  - compute determinant of the deformation tensor $J_n = \det \mathbf{F}_n$
  - compute Cauchy-Green deformation tensor $\mathbf{C}_n = \mathbf{F}_n^{\mathrm{T}}\mathbf{F}_n$
  - spectral decomposition $\mathbf{C}_n = \sum_{A=1}^{3} \lambda_{A\,n}^2\, {}^0\mathbf{N}^{(A)}\, {}^0\mathbf{N}^{(A)\ \mathrm{T}}$
  - logarithmic strain tensor $\ln \mathbf{U}_n = \sum_{A=1}^{3} \ln \lambda_{A\,n}\, {}^0\mathbf{N}^{(A)}\, {}^0\mathbf{N}^{(A)\ \mathrm{T}}$
  - inverse right stretch tensor $\mathbf{U}_n^{-1} = \sum_{A=1}^{3} \lambda_{A\,n}^{-1}\, {}^0\mathbf{N}^{(A)}\, {}^0\mathbf{N}^{(A)\ \mathrm{T}}$
  - compute rotation tensor $\mathbf{R}_n = \mathbf{F}_n\mathbf{U}_n^{-1}$
  - compute logarithmic stress $\mathbf{T}_n = 2\mu \ln \mathbf{U}_n + \Lambda \ln J_n\, \mathbf{I}$
  - compute Cauchy stress tensor $\boldsymbol{\sigma}_n = J_n^{-1}\mathbf{R}_n\mathbf{T}_n\mathbf{R}_n^{\mathrm{T}}$
  - compute strain-displacement matrix ${}^t\mathbf{B}_n^{(e)}$
  - $\mathbf{f}_{\text{int}} \leftarrow \mathbf{f}_{\text{int}} + \alpha\, {}^t\mathbf{B}_n^{(e)\,\mathrm{T}}\boldsymbol{\sigma}_n$ (where α is the weighting factor for given Gauss point)

BOX 1:

The nonlinear equation system

$$\mathbf{g} = \mathbf{0} \tag{7}$$

can be solved by iteration. The most frequently used and the most robust method for the solution of (7) is the Newton-Raphson iteration method. The iteration schemes for Newton-Raphson solution method is based on a Taylor series expansion of the residual vector in the neighbourhood of the point $\mathbf{u}_n$

$$\mathbf{g} = \mathbf{g}(\mathbf{u}_n) + \left.\frac{\partial \mathbf{g}}{\partial \mathbf{u}}\right|_{\mathbf{u}_n} (\mathbf{u} - \mathbf{u}_n) + \text{ higher-order terms} = \mathbf{0} \tag{8}$$

Neglecting the higher-order terms and denoting the current tangent stiffness matrix

$$\mathbf{K}_n = \left.\frac{\partial \mathbf{g}}{\partial \mathbf{u}}\right|_{\mathbf{u}_n} \tag{9}$$

we can calculate an increment in the displacement $\Delta\mathbf{u}_{n+1} = \mathbf{u}_{n+1} - \mathbf{u}_n$ from the relation

$$\mathbf{K}_n \Delta\mathbf{u}_{n+1} = -\mathbf{g}(\mathbf{u}_n) \tag{10}$$

A characteristic of the Newton-Raphson iteration is that the new tangent stiffness matrix is calculated in each iteration. However this method is very expensive for large-order systems, the solution cost can be reduced significantly by employing the quasi-Newton methods based on Newton-Raphson method without the explicit re-formation of the tangent stiffness matrix. Instead of calculating the tangent stiffness $\mathbf{K}_n$ we can use the initial stiffness matrix and update only the residual vector in every iteration. This method is called a initial stress method and may converge very slowly or even diverge. Among the quasi-Newton methods available, the BFGS method appears to be most effective, because does not destroy the banded nature of the finite element stiffness matrix.

BFGS

The BFGS method (called after Broyden, Fletcher, Goldfarb and Shanno) involve updating the coefficient matrix to provide a secant approximation to the matrix. The algorithm is described in [Matthies and Strang 1979] or in [Bathe 1996]. For a given approximation $\mathbf{u}_n$ of the solution $\mathbf{u}$, the algorithm will choose a search direction $\mathbf{d}_n$, in which the line search is applied to find a better approximation.

The important point is the choice the direction $\mathbf{d}_n$. The idea of Davidon is to update the stiffness matrix $\mathbf{K}$ in a simple way after each iteration, rather than to recompute it entirely (full Newton-Raphson method) or leave it unchanged (initial stress method). The update formula of the stiffness matrix for the BFGS method must satisfy four requirements:

1. The new matrix $\mathbf{K}_n$ should satisfy the quasi-Newton equation

$$\mathbf{K}_n \boldsymbol{\delta}_n = \boldsymbol{\gamma}_n \tag{11}$$

where $\boldsymbol{\delta}_n$ denotes a displacement increment

$$\boldsymbol{\delta}_n = \mathbf{u}_n - \mathbf{u}_{n-1} \tag{12}$$

and $\boldsymbol{\gamma}_n$ is the increment of the residual force vector

$$\boldsymbol{\gamma}_n = \mathbf{g}_n - \mathbf{g}_{n-1} \tag{13}$$

2. If $\mathbf{K}_{n-1}$ is symmetric, then the new $\mathbf{K}_n$ should be also symmetric. This is automatically fulfilled if the residual $\mathbf{g}$ is a gradient of some scalar potential.

3. If $\mathbf{K}_{n-1}$ is positive definite, then the new $\mathbf{K}_n$ should also be positive definite.

4. The new search direction $\mathbf{d}_n = \mathbf{K}_n^{-1}\mathbf{g}_n$ should be inexpensive to compute.

The last condition is the essential point. It is accomplished by requiring that $\mathbf{K}_n$ should differ from $\mathbf{K}_{n-1}$ only by a matrix of very low rank. Our favorite, which satisfies also the conditions 1–3, is a correction of rank two. Conveniently this update is written in terms of $\mathbf{K}_{n-1}^{-1}$ rather than $\mathbf{K}_{n-1}$. This inverse also differs from its predecessor by a matrix of rank 2, and the correction can be put into product form

$$\mathbf{K}_n^{-1} = \mathbf{A}_n^{\mathrm{T}}\mathbf{K}_{n-1}^{-1}\mathbf{A}_n \tag{14}$$

with

$$\mathbf{A}_n = \mathbf{I} + \mathbf{v}_n\mathbf{w}_n^{\mathrm{T}} \tag{15}$$

We can see immediately that the requirements of symmetry and positive definiteness are achieved.

Vectors $\mathbf{v}_n$ and $\mathbf{w}_n$ are set to satisfy the quasi-Newton equation (11). Thus

$$\begin{aligned} \mathbf{v}_n &= -\sqrt{\frac{\boldsymbol{\delta}_n^{\mathrm{T}}\boldsymbol{\gamma}_n}{\boldsymbol{\delta}_n^{\mathrm{T}}\mathbf{K}_{n-1}\boldsymbol{\delta}_n}}\,\mathbf{K}_{n-1}\boldsymbol{\delta}_n - \boldsymbol{\gamma}_n \\ \mathbf{w}_n &= \frac{\boldsymbol{\delta}_n}{\boldsymbol{\delta}_n^{\mathrm{T}}\boldsymbol{\gamma}_n} \end{aligned} \tag{16}$$

To avoid the numerically dangerous updates we have to evaluate the condition number c of the updating matrix $\mathbf{A}_n$. It is defined as an absolute value of the ratio of the maximum and minimum eigenvalues. The eigenvalues of matrix $\mathbf{A}_n$ are (in ascending order) $\lambda_1 = \lambda_2 = \ldots = \lambda_{N-1} = 1$ and $\lambda_N = 1 + \mathbf{w}_n^{\mathrm{T}}\mathbf{v}_n$, where N is an order of the matrix $\mathbf{A}_n$. Then

$$c = \left|\frac{\lambda_N}{\lambda_1}\right| = \left|1 + \mathbf{w}_n^{\mathrm{T}}\mathbf{v}_n\right| \tag{17}$$

Substitution of (16) into (17) we obtain the relation from which the condition number is calculated in the FEM program

$$c = \sqrt{\frac{\beta_0\, G(0)}{G(0) - G(\beta_0)}} \tag{18}$$

For $G(\beta) \to G(0)$ there is no reduction in residual, $c \to \infty$, which means that the structure is unstable and updates to the secant matrix $\mathbf{K}_n$ should be avoided. The critical value of c is taken as 5.

BFGS iteration schemes

- initialization of the iteration process
  - initial displacements $\mathbf{u}_0 = \mathbf{0}$
  - initial tangent stiffness $\mathbf{K}_0$, usually the elastic matrix $\mathbf{K}_0 = \mathbf{K}_\mathrm{e}$
  - initial residual $\mathbf{g}_0$ is prescribed right hand side $\mathbf{g}_0 = -\mathbf{f}_\mathrm{ext}$
  - calculate $\mathbf{K}_0^{-1}$ from the triangular factorization of $\mathbf{K}_0$
  - find search directions $\mathbf{d}_0$ from $\mathbf{d}_0 = -\mathbf{K}_0^{-1}\,\mathbf{g}_0$
  - define $G(0) = \mathbf{d}_0^\mathrm{T}\mathbf{g}_0$
  - line search in the direction $\mathbf{d}_0$: find the optimum value of β_0 minimizing the scalar function $G(\beta_0) = \mathbf{d}_0^\mathrm{T}\mathbf{g}(\mathbf{u}_0 - \beta_0\,\mathbf{d}_0)$
  - evaluate condition number $c = \sqrt{\frac{\beta_0 G(0)}{G(0)-G(\beta_0)}}$. If $c > 5$ the update is not performed
  - new approximation of solution $\mathbf{u}_1 = \mathbf{u}_0 - \beta_0\,\mathbf{d}_0$
  - new residual $\mathbf{g}_1 = \mathbf{g}(\mathbf{u}_1)$
- do for $n = 1, 2, 3\ldots$ while prescribed accuracy is not achieved
  - $\boldsymbol{\delta}_n = \mathbf{u}_n - \mathbf{u}_{n-1}$
  - $\boldsymbol{\gamma}_n = \mathbf{g}_n - \mathbf{g}_{n-1}$
  - $\mathbf{v}_n = -\sqrt{\frac{\boldsymbol{\delta}_n^\mathrm{T}\boldsymbol{\gamma}_n}{\boldsymbol{\delta}_n^\mathrm{T}\mathbf{K}_{n-1}\boldsymbol{\delta}_n}}\,\mathbf{K}_{n-1}\boldsymbol{\delta}_n - \boldsymbol{\gamma}_n$
  - $\mathbf{w}_n = \frac{\boldsymbol{\delta}_n}{\boldsymbol{\delta}_n^\mathrm{T}\boldsymbol{\gamma}_n}$
  - update of the stiffness matrix $\mathbf{K}_n^{-1} = (\mathbf{I} + \mathbf{w}_n\mathbf{v}_n^\mathrm{T})\mathbf{K}_{n-1}^{-1}(\mathbf{I} + \mathbf{v}_n\mathbf{w}_n^\mathrm{T})$
  - search direction $\mathbf{d}_n = \mathbf{K}_n^{-1}\,\mathbf{g}_n$
  - line search in the direction of $\mathbf{d}_n$: find the optimum value of β_n minimizing the scalar function $G(\beta_n) = \mathbf{d}_n^\mathrm{T}\mathbf{g}_n$
  - calculate condition number $c = \sqrt{\frac{\beta_n G(0)}{G(0)-G(\beta_n)}}$. If $c > 5$ the update is not performed
  - new approximation of the solution $\mathbf{u}_{n+1} = \mathbf{u}_n - \beta_n\,\mathbf{d}_n$
  - new residual $\mathbf{g}_{n+1} = \mathbf{g}(\mathbf{u}_{n+1})$
  - check of convergence - if $\|\mathbf{u}_{n+1} - \mathbf{u}_n\| < \mathsf{UTOL}\,\|\mathbf{u}_{n+1}\|$ and $\|\mathbf{g}_{n+1}\| < \mathsf{RTOL}\|\mathbf{g}_0\|$ then quit
- end of the loop

BOX 2:

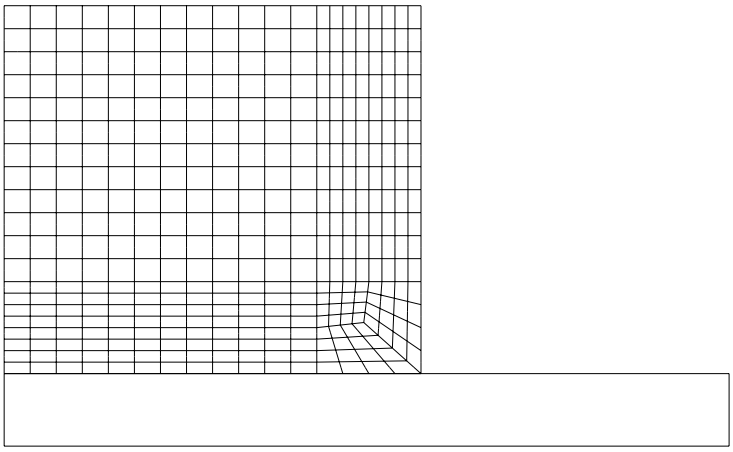

Figure 1: FEM model of the quarter of the cross-section of the cylindrical specimen used in compression test.

The algorithm of the BFGS method is fully described in the Box 2.

The advantage of the algorithm is that the number of auxiliary vectors $\mathbf{v}_n$, $\mathbf{w}_n$ can be kept reasonably small, say 10-15. Than the vectors can be abandoned and the iterations recommenced from the new point $\mathbf{u}_n$ but with the same initial matrix $\mathbf{K}_0$.

4. Numerical example

The described algorithm was used for numerical simulations of the compression test of the rubber cylinder. During the deformation, the stress field is not uniaxial - even if heads of the testing machine are greased, they prevent extension of the diameter of the cylindrical specimen on the pressure heads. This is the reason why the experimental data cannot be compared with the analytical solution but the numerical simulation has to be carried out.

The compression of the cylindrical specimen is from a nature an axisymmetric task, which is even symmetric to the plane parting the cylinder to two of half length. Thus the FEM task is also axisymmetric, the finite element model is shown in the Fig. 1. The model consist of 384 eight nodes axisymmetric elements. The quadratic elements are used because of the higher accuracy obtained with lower computational costs. The pressure head of the testing machine is modelled by one axisymmetric element.

Adequate boundary conditions agreeing with the experimental conditions was prescribed. All nodes in the plane of symmetry were prevented moving in the axial direction. Because of the friction between the specimen and the pressure head of the testing machine, the radial displacements of the nodes of the specimen in the pressed plane were prescribed to be zero. The displacement loading was prescribed in the nodes on the pressed plane, namely in every node was prescribed in the axial direction a spring with stiffness 10^{11} Nm^{-1} and the additional force which cause the required axial displacement.

The stiffness of the spring is five orders higher than the stiffness of the material, which is sufficient and at the same time it avoids the numerical difficulties produced by two different materials with too different stiffness.

To avoid the rolling of the rubber material over the edge of the cylinder, one element representing the pressure head was added to the FEM model. Then it is possible to prescribe the contact between the pressure head and the wall of the cylindrical specimen. In all nodes belonging to the element representing pressure head was prescribed identical displacement load like in the nodes in the pressed cross-section of the cylinder.

For the modelling of constitutive relations the logarithmic formulation was used. The only material parameter which represents the shear modulus is μ. Its size for the soft rubber used for compression test and tension test was derived from the tension characteristic and it is $\mu = 1.4$ MPa. For the second material used to the compression test II and shear test was its size determined from the measured shear characteristic and it is $\mu = 1.12$ MPa. Because the rubber material is nearly incompressible, the Poisson's ratio used in computations was set $\nu = 0.49$.

If the specimen is compressed to approximately 70% of it original length, the lateral surface of the cylindrical wall of the specimen and the surface of the element corresponding to the pressure interface together and the contact computations must be carried out.

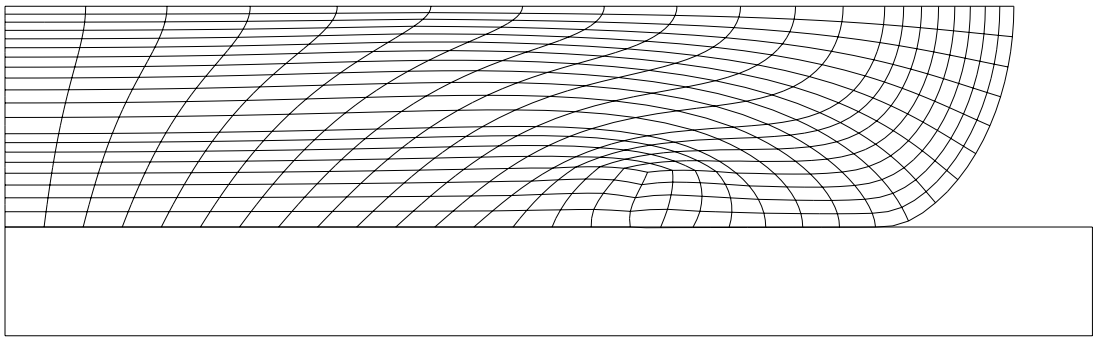

Figure 2: Deformed mesh for 60% compression.

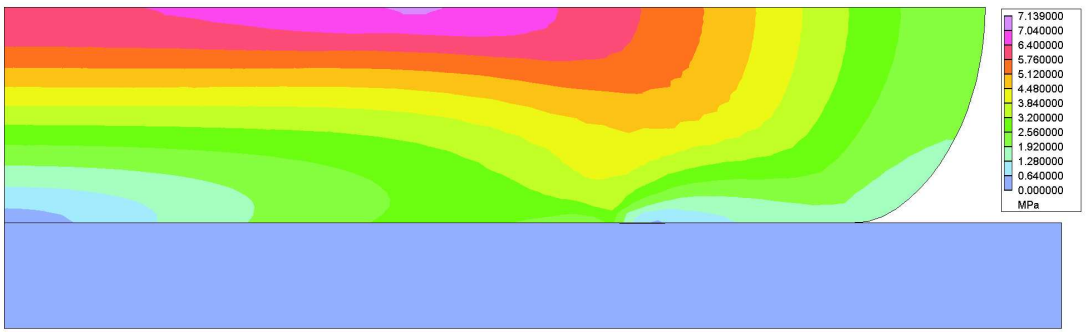

Figure 3: Von Mises stress on the deformed mesh, 60% compression.

The deformed mesh obtained from the numerical simulation is plotted in Fig. 2. The distribution of the Von Mises stress on the deformed specimen for the compression to the 40% of its original length is given in the Fig. 3. The importance of the prescription of contact between the lateral surface of the cylindrical specimen and the element representing the pressure head is obvious.

With the mesh used for the computations, it is not possible to reach much larger compressions that it is shown in Fig. 2. The reason is that the distortion of elements in the upper part of the model is too big, the ratio between the two sides of quadrilateral elements is too high.

5. Acknowledgements

This work was sponsored by the Grant Agency CR under project No. 101/03/0331.

6. References

Poživilová, A. (2002) *Constitutive modelling of hyperelastic materials using the logarithmic description* Ph.D. Thesis, CTU Prague.

Poživilová, A. and Plešek, J. (2002) Elastomery, konstitutivní modelování, identifikace materiálových parametru a porovnání s experimentem, *Proceedings of Engineering mechanics 2002* Svratka

Matthies H. and Strang G. 1979 The solution of nonlinear finite element equations. *International Journal for Numerical Methods in Engineering*, Vol. 14, pp. 1613—1626.

Bathe K. J. (1996) *Finite element Procedures*, Prentice Hall, New Jersey.